Review of dark matter and detect dark matter using collider

Ning Yan

Department of Physics and Astronomy, York University, Toronto, M3J 1P3, Canada

yn604332298@gmail.com

Abstract. This review study will give a brief introduction to dark matter, Large Hadron colliders (LHC), and circular electron-positron colliders(CEPC). The first part of the paper will discuss the fundamental properties of dark matter and the evidence for its existence. There will be a brief discussion of the theories used to explain dark matter. There will be three dark matter profiles and dark halo introductions. The basic configuration, ideas, and dark matter detection of LHC will then be covered in the study. The detection process includes missing momentum signals, bump hunting, and limiting the WIMP zone. The final section will describe CEPC's basic setup and its benefits for locating dark matter.

Keywords: dark matter, dark matter detection, LHC, CEPC.

1. Introduction

By hypothesis, dark matter is matter that doesn't interact with any electromagnetic field. The word 'dark' means it is tough to detect because dark matter doesn't interact with electromagnetic radiation. According to NASA Science, dark matter makes up 85% of the universe's mass, whereas conventional matter makes up only 5% of the cosmos. Dark energy makes up the remaining 68%. [1]

In 1884, by calculating the observed velocity dispersion of the stars orbiting around the galaxy's center, Lord Kelvin first invented the idea of dark bodies [2]. By analyzing the velocity of stars, Dutch astronomer Jacobus Kapteyn initially hypothesized the presence of dark matter in 1922 [3]. Because many of the current astrophysical observations cannot be explained unless assuming the existence of dark matter, thus scientist today believes that dark matter is abundant and has had a strong influence [4].

A galaxy rotation curve is an excellent way to comprehend the justifications for dark matter's existence. In 1959, Louise Volders pointed out that spiral galaxy M33 doesn't follow Keplerian dynamics [5]. This result has been expanded to many other spiral galaxies before 1978 [6]. The Newtonian dynamics predict that the radial density profile $\rho(r)$ is:
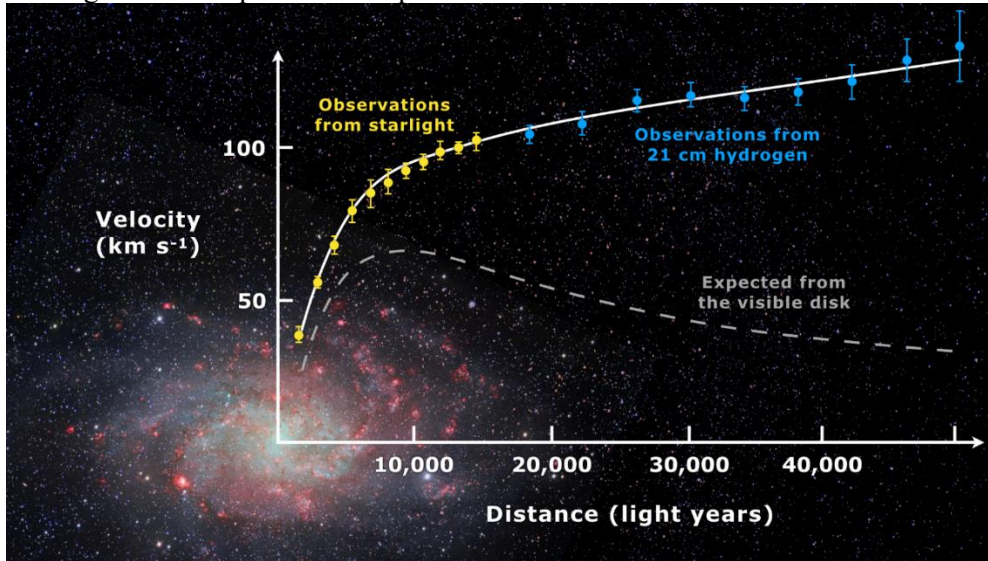
$$\rho(r) = \frac{v(r)^2}{4\pi G r^2}\left(1 + 2\frac{d\log v(r)}{d\log r}\right) \qquad (1)$$

Where $v(r)$ is the radial orbital velocity profile, G stands for the widely recognized gravitational constant. Based on this model, the orbit of matter in spiral galaxies should be like planets in the solar system. Thus, the average orbital speed should decrease according to the density profile and be proportional to the inverse square of the distance from the galaxy's center. In 1975, Vera Rubin and Kent Ford discovered that most of the stars in the galaxy roughly have the same orbital speed, which doesn't fit the prediction of Newtonian dynamics [7]. This observation suggests that the spiral galaxy has nearly

linear masses growing concerning distance. The observed average orbit velocity in spiral galaxies indicates that:
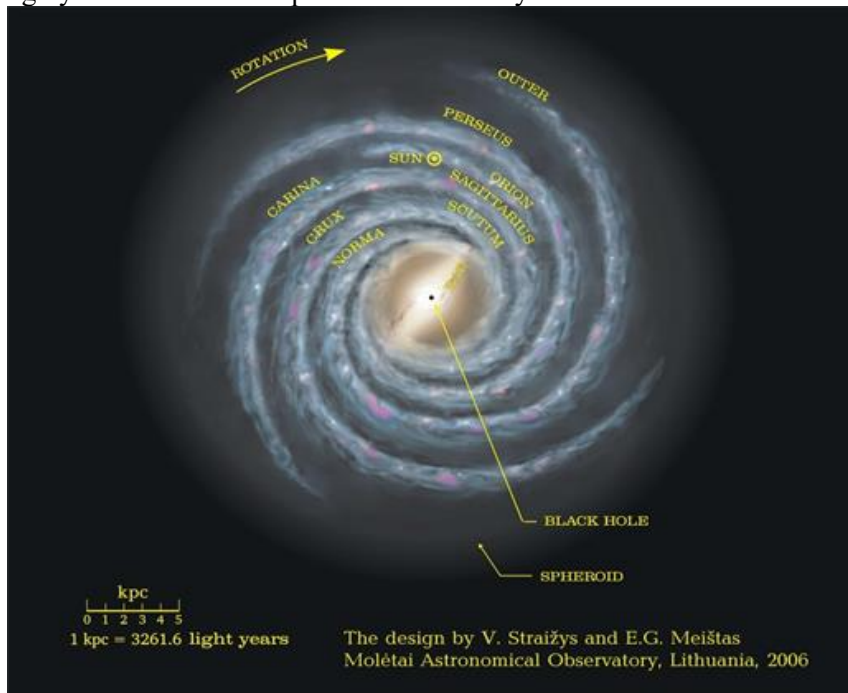
$$v(r) = \left(r\frac{d\Phi}{dr}\right)^{\frac{1}{2}} \tag{2}$$

Where Φ is the gravitational potential of the galaxy and v is the orbit's average measured velocity. And $\Phi = \frac{U}{m}$, where U is the gravitational potential energy, m is the mass, and the unit is work per unit mass, gives the gravitational potential at a place.

Figure 1. Rotation curve of M33 spiral galaxy [8].
Note: The yellow and blue points are observations with error bars. The grey line is the line that fits data points best. The grey dashed line is the prediction with only visible matter counts.
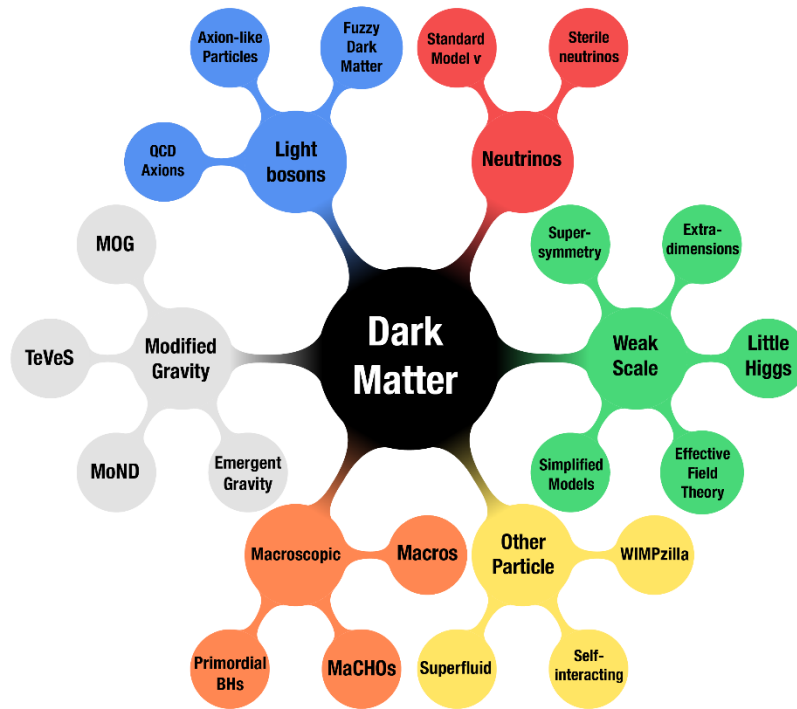

Figure 2. Rotation of the Milky Way [9].
An illustration of the M33 spiral galaxy's rotation curve is shown in Figure 1. The Newtonian

dynamics forecast is shown as a grey dashed line using observable stuff. The predicted velocities start to decrease from 10,000 light years. But the observations are more like a mono-increasing function concerning distance.

Figure 2 shows how the Milky Way's arms rotate through several stages. About the Milky Way's center, the components of the galaxy revolve clockwise. If dark matter doesn't exist, then the sun should escape from Milky Way because there aren't enough matters to provide sufficient gravity force. Given that the sun maintains its orbit, gravity must be produced by some invisible substance, which raises the likelihood of dark matter.

Additional proof exists for the existence of dark matter. In 2006, Douglas Clowe claimed that he used Chandra X-ray Observatory to direct detected dark matter while observing the galaxy cluster 1 E 0657-558 [10].

Figure 3. The theories of dark matter [11].

Figure 3 provides the hypothesis of dark matter. There are various theories about dark matter. It can be classified as light bosons, neutrinos, weak scale, other particles, macroscopic, and modified gravity (MOG). Any case interacting with visible matter significantly qualifies as dark matter, according to its characteristics. It doesn't necessarily mean dark matter cannot at least partially consist of ordinary baryonic matter, but none of the fundamental particles are good candidates for dark matter.

Dark matter is not evenly distributed all around space. They are dispersed in what is known as dark matter halos. A variety of density patterns has described the structure of dark matter halos. One standard model is the pseudo-isothermal halo:[12]

$$\rho(r) = \frac{\rho_0}{1+\left(\frac{r}{r_c}\right)^2} \tag{3}$$

Where r_c is the core radius and ρ_0 is the finite central density.

Navarro-Frenk-White (NFW) profile: [13]

$$\rho(r) = \frac{\rho_{crit}\delta_c}{\left(\frac{r}{r_s}\right)\left(1+\frac{r}{r_s}\right)^2} \tag{4}$$
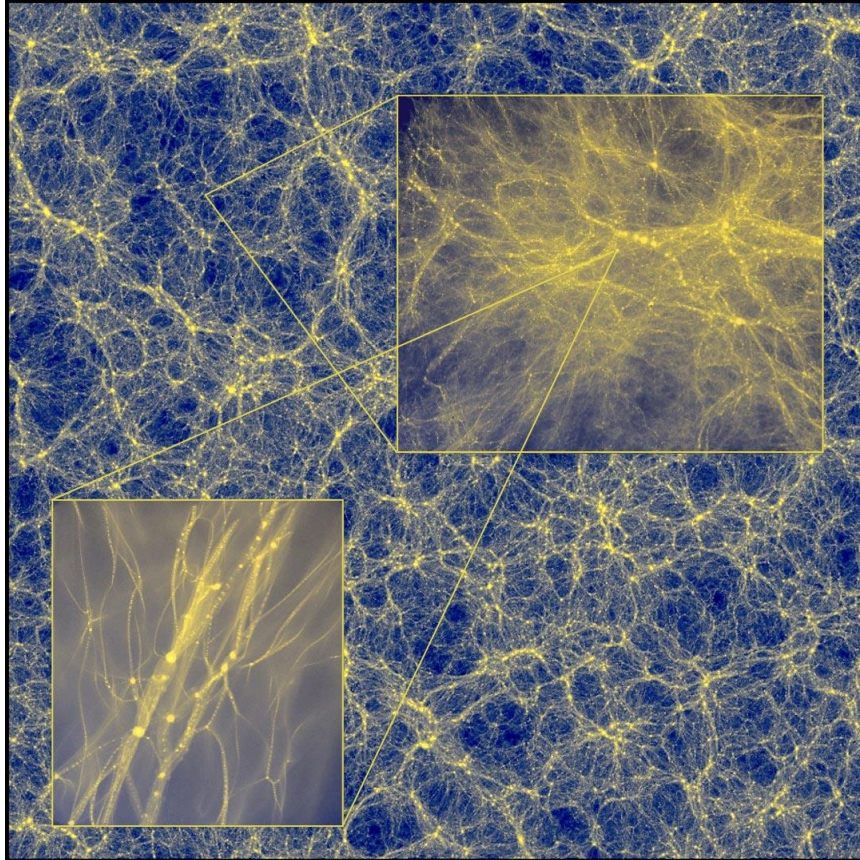
Where $\rho_{crit} = \frac{3H^2}{8\pi G}$ is the critical density for closure, δ_c is characteristic density, and r_s is scale radius.

Einasto profile: [14]

$$\rho(r) = \rho_e e^{-d_n\left(\left(\frac{r}{r_e}\right)^{\frac{1}{n}}-1\right)} \tag{5}$$

Where r is the spatial radius, r_e is the radius that volume contains half of the total mass, ρ_e is the density at radius r_e, and d_n is the function of n.

None of these profiles can completely capture all dark matter halos' characteristics. Dark matter in the galaxy is frequently referred to as the pseudo-isothermal halo. It also brings an excellent fit to many rotation curves but got an infinity radius when enclosed mass doesn't converge to a finite value. NFW profile provides good fits for many halo masses but is only suitable for isolated halos. [15,16]. NFW halos have poor performance predicting galaxy data compared to pseudo-isothermal profiles, which leads to the so-called cuspy halo problem. Einasto's profile is better at describing higher-resolution computer simulations. Even though Einasto shape doesn't significantly differ from NFW halos, it will still lead to a cuspy halo problem.

Note: The distance between the two sides of a computer-generated simulation of the distribution of dark matter in the universe is 2.4 billion light years. The diagram shows two zoom-in processes. The top right is the dark matter halo with a million years across. The bottom left is a zoom-in of the top right, a dark matter halo of Earth-size.

Figure 4. Zooming in on Dark Matter distribution [17].

A more concrete understanding of the distribution of dark matter may be gained from Figure 4, which represents a computer simulation of dark matter in the cosmos if observed. The blue regions are empty spaces or visible matter; the yellow areas are dark matter. It is simple to see that dark matter is not

dispersed equally but like capillaries.
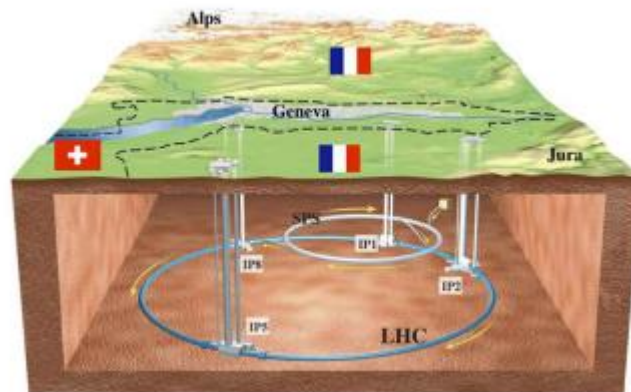
2. Detect dark matter

In modern particle physics and astrophysics, the detection of dark matter is a very active study area and is crucial. There are majorly three approaches to detecting dark matter: 1. Direct detection approach; 2. Indirect detection approach; 3. Collider approach.

Direct detection is trying to measure the existing dark matter. Since dark matter is heavily distributed in the universe, Earth must intercept some dark matter while orbiting the Sun and the Milky Way. Thus, direct detection aims to capture these dark matters passed by the Earth. To make a precision measurement, it is crucial to lower the background, especially the cosmic ray and gamma background. [18] Thus, the laboratory for detecting dark matter is usually deep underground such as the 2500-meter-deep China Jinping Underground Laboratory [19]. Indirect detection of dark matter differs from direct detection in that it looks for the outcomes of dark matter interactions rather than the dark matter itself [20]. Dark matter can interact in two different ways: annihilating and decaying. For instance, dark matter might yield gamma- or antiparticle pairs after destruction [21]. And dark matter could decay into standard model particles or other particles. The destruction and decay process can be indirectly detected by measuring the gamma-ray, antiprotons, or positrons [22].
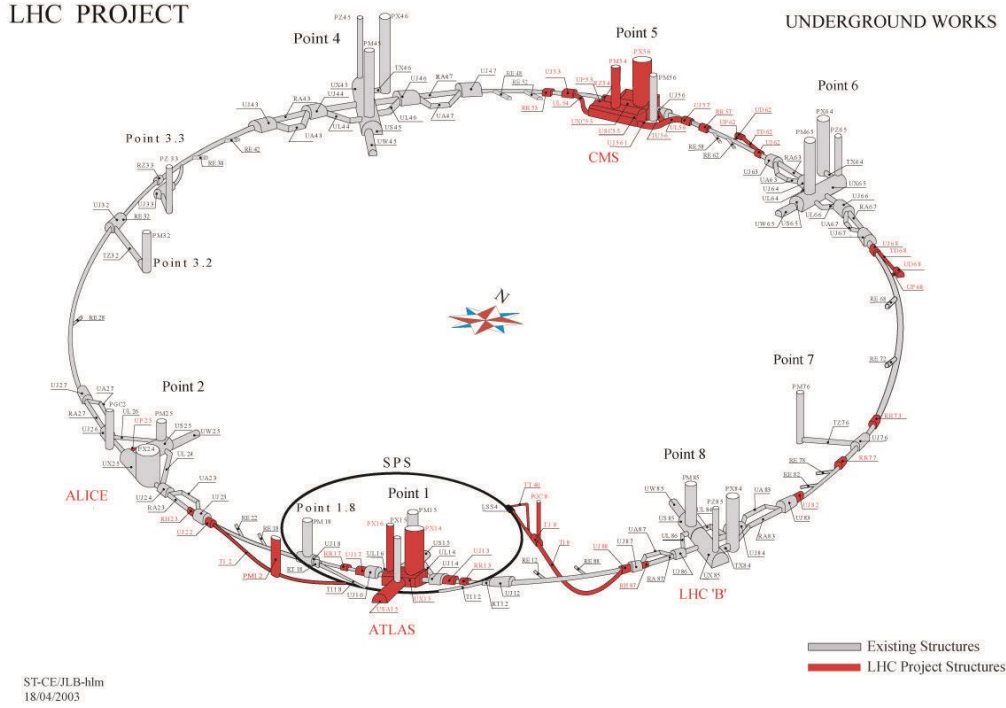
The third approach is collider searches. This approach tries to produce dark matter using colliders [23]. The Large Hadron Collider (LHC) and Circular Electron Positron Collider (CEPC) are two candidates to have dark matter as a collider. The following section will introduce these two colliders in detail.

3. LHC and dark matter detection

LHC is a proton-proton collider with two rings. It is superconducting. The 27 km long tunnel was built to house a sizeable electron-positron collider (LEP). According to figure 5, the tunnel is installed underground.
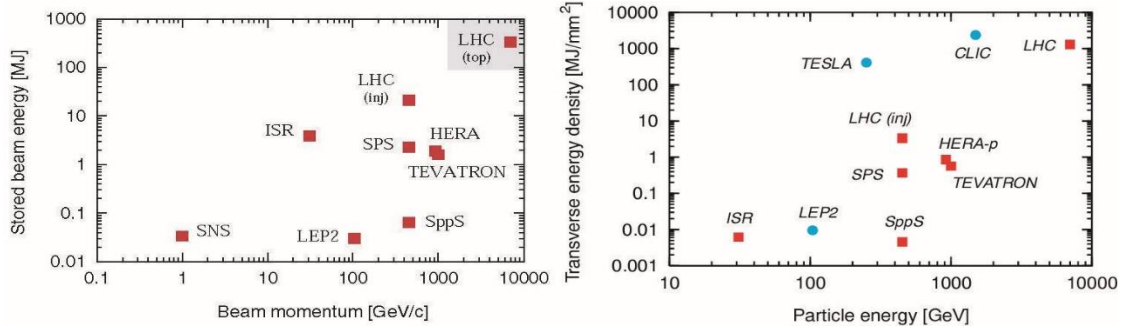

Figure 5. Four interaction areas and the LHC collider are shown schematically [24].

Figure 6. Schematic layout of the LHC with eight arc sections [25].

As shown in figure 6, there are eight arcs and eight 528 meters straight sections in LHC. The LHC's two beam pipes cross four interaction zones. The LHC detectors are divided into eight consecutive parts with radio frequency, machine utilities, beam abort, and collimation.

Note: The left is beam energy concerning the momentum of various colliders. The right is beam energy densities concerning the rate of multiple colliders.

Figure 7. Comparison of LHC with other Previous Colliders [25].

At nominal luminosity, each beam stored energy of more than 350 MJ. Figure 7 illustrates how the LHC has more energy stored than any other collider by more than two orders of magnitude and more energy density by three orders of magnitude. The number of collisions per second caused by beam-beam collisions is calculated as follows: [26]

$$\dot{n} = L\sigma \tag{6}$$

Where L is the luminosity and σ is the cross-section. The unit of cross sections is b (barn) and $1b = 10^{-24}cm^2$. Luminosity is determined by geometry and particle flux and given by: [26]

$$L = \frac{N_1 N_2 n_b f_{rev}}{A} \tag{7}$$

N_1 is the number of particles per bunch in beam 1, and N_2 is the number of particles per bunch in beam 2. n_b is the total number of bunches, f_{rev} is the revolution frequency, and A is the beam overlap

cross-section area. For beam size σ_x and σ_y, $A = \pi\sigma_x\sigma_y$, if beams are Gaussian shaped.

Before the collision, the beam should be concentrated into as small a transverse beam size as possible to focus the crash and get high luminosities. It requires nearly 3000 bunches, and a magnetic field is needed to focus the system at top energy. It is called beam squeezing. The formula for the r.m.s beam size at point s is [26]

$$\sigma(s) = \sqrt{\epsilon\beta(s)} \qquad (8)$$

where ϵ denoted emittance, refers to the beam size in transverse phase space and is an average beam quantity.

The primary objective of LHC is to investigate the Standard Model. Electron-positron collisions took place in LEP in 1989. However, the discussion of LHC starts as early as 1983 [27]. In the later ten years, the competition between LHC and SSC projects pushed LHC design parameters significantly evolved [28]. During the last ten years, LHC has started hunting dark matters [29].

One way to achieve that is by using a missing momentum signal [30]. Since the dark matter has little interaction with ordinary matter, if a collision makes dark matter, then the total momentum after the crash should decrease. This is because some rates are missing for the dark matter produced, which can't be observed [31]. The dark matter escaped from LHC unnoticed.

For simplified models, there is a different way called bump hunting. Bump hunting pays attention to a bump in a smooth background of events in the collision. For example, the researcher can search for stop quark pairs, which can bump hunting with a single entry per event.

The LHC also restricted the possible conditions for WIMP. The researchers at LHC failed to find any evidence of dark matter directly. However, the territory of WIMP is significantly narrowed, including their masses and interaction strengths [29].
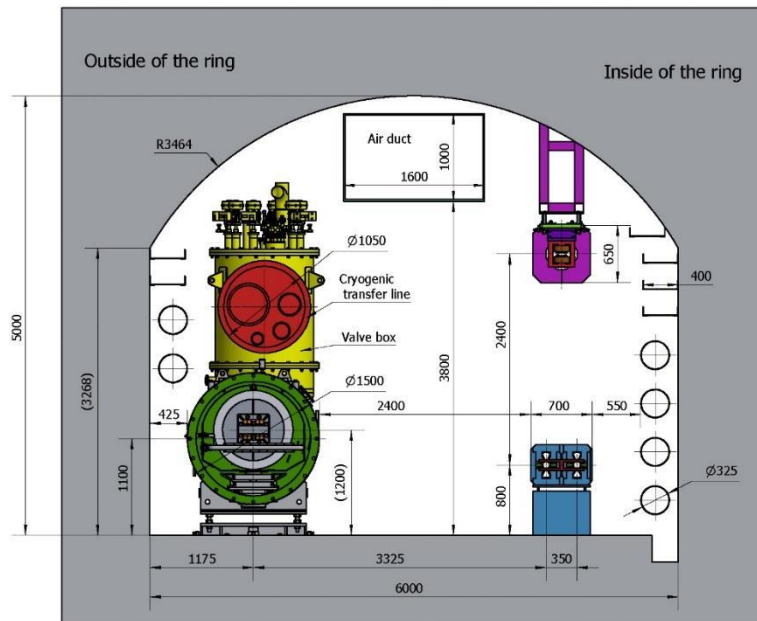
4. CEPC and dark matter detection

Colliders of various types, including proton-proton, proton-antiproton, electron-positron, electron-proton, electron-ion, and ion-ion colliders, have been constructed throughout the past few decades. These colliders are critical in rounding out the Standard Model's constituent parts. The finding of the Higgs boson at the LHC in 2012 is a prime illustration [32]. The colliders are thus called "engines of discovery."

The Higgs boson weighs roughly 125 GeV, a relatively small mass. To study new particles, greater accuracy is needed. The synchrotron radiation from the high-energy electron and positron beams must be reduced. Hence the collider's ring must have a big radius to do this. A large e^+e^- circular collider can provide higher luminosity than a linear collider.
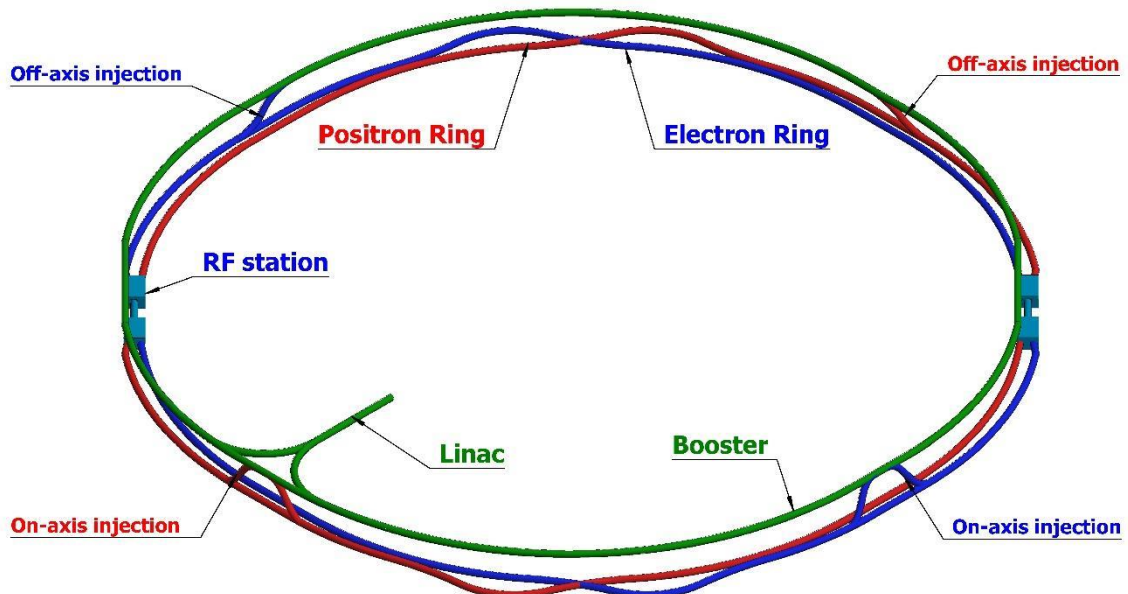
The Chinese Academic Society's Institute of High Energy Physics began researching CEPC shortly after the Higgs Boson was discovered at CERN in 2012. The designed center of mass for CEPC is 240 GeV. The CEPC will be able to operate at 91 GeV as a Z factory or 160 GeV as a W factory as well.

The Booster, the Collider, the Linear Accelerator, the Damping Ring, and a few Transport Lines make up the CEPC. The 100 km-long underground tubes will house the booster and collider rings.
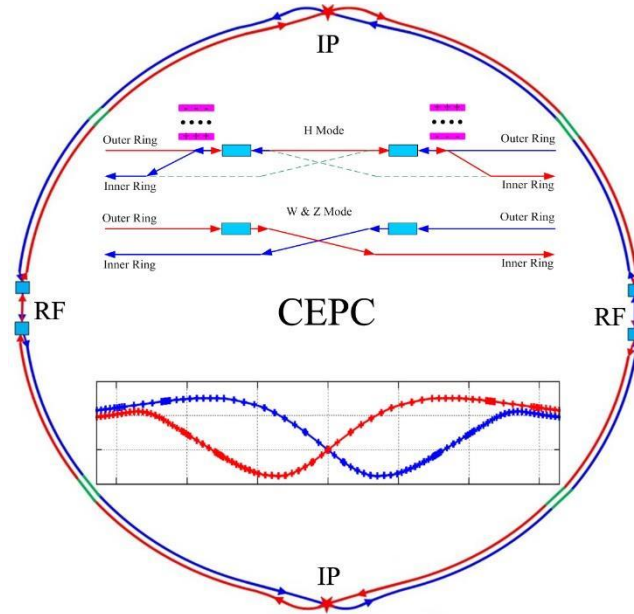
Figure 8. Tunnel cross-section for CEPC [33].

Figure 8 illustrates a cross-section of the CEPC tunnel. To prevent interference between the collider and the rocket, the booster is located 2.4 m above the collider.
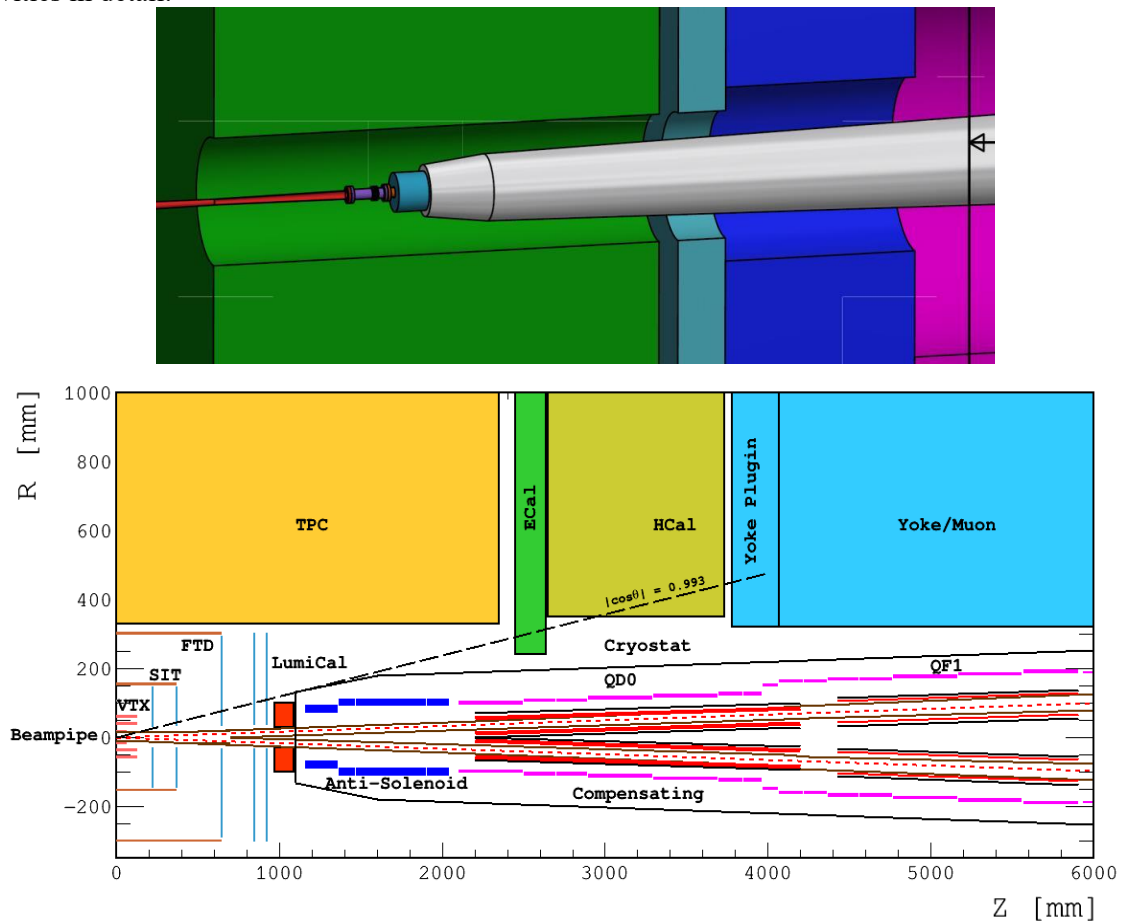

Figure 9. Design of CEPC [33].

Figure 9 depicts the CEPC and Linear Collider configuration and the transfer lines, Booster, and Collider. The 1.2 km long linear collider is located on the ground. The Booster is situated 100 meters below ground. The Collider has four injection zones, 2 RF, and two interaction regions.

Figure 10. Layout of CEPC Collider [33].

As shown in figure 10, the layout of the Collider. Moreover, it illustrates the superconducting RF cavities in detail.

Figure 11. The Interaction Zone's Center [33].

The interaction region's core portion is seen in figure 11. The Be pipe is 14 cm long and has an inner radius of 14 mm. The focusing magnets are 2.2 m away from the interaction points.

The CEPC has two interaction points and a double ring. It is designed to have three different modes. The CEPC is a double-ring e+e collider with two interaction locations and a 100-kilometer radius (IP). Concerning three different center-of-mass energies, it will operate in three different modes: the Higgs factory at $\sqrt{s} = 240$ GeV, the Z factory at $\sqrt{s} = 91.2$ GeV, and the WW threshold at $\sqrt{s} \approx 160$ GeV. [34]
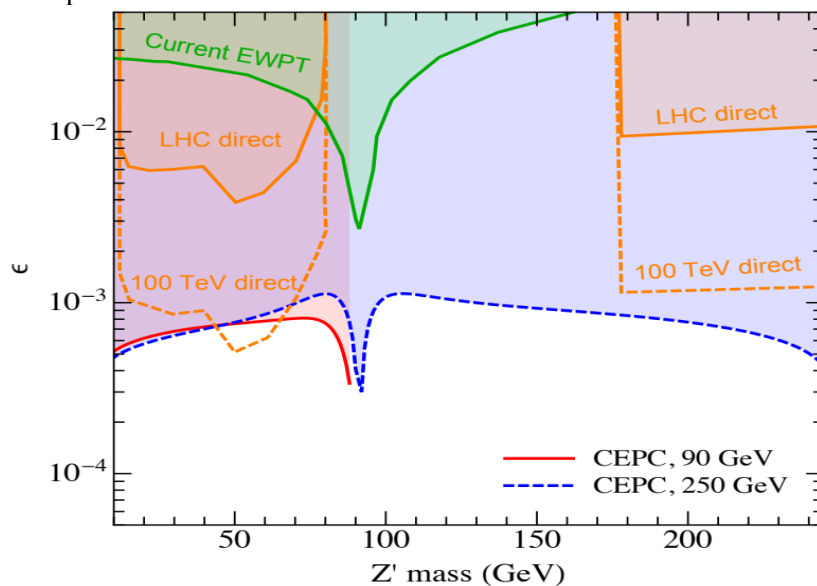
High precision is required for producing new physics and filling out and testing the Standard Model. These specifications form the basis of the CEPC detector's design. The energy resolution of the CEPC needs to improve to another level over today's limit. Thus, two primary detector concepts were studied to achieve this goal. The first involved a baseline detector concept with two tracking system approaches. The particle flow theory is used in this basic detector design. The second was another strategy for meeting the jet resolution requirements. It uses a complete silicon tracker. Each detector subsystem is in R&D and will provide more advances in detector science.

After the activation of the accelerator and detectors, CEPC construction is anticipated to be completed in 2030. The tentative operational schedule for the ten years is as follows: one year for the WW threshold scan, seven years for the Higgs boson, and two years for the Z pole.

There are two models of electroweak dark matter, the doublet–singlet and doublet–triplet models. The strength of CEPC is electroweak physics. The capabilities of CPEC for electroweak physics are limited. [35-37] Thus, it is very natural for CEPC searches electroweak multiples dark matter particle [38]. CEPC could help to investigate the properties even if a direct detection experiment made the discovery. Two possibilities exist for an electroweak dark matter missed by natural detection experiments but detected by CEPC. The first scenario is that dark matter is almost purely electroweak multiplet, which weakly interacts with the Higgs boson and could hardly be measured by LHC [39]. The second possible explanation is a mixed electroweak multiplet of dark matter with connections to the Higgs boson.

The dark matter may interact with the SM particles through gauge-invariant "portal" operators even if it does not exist in an electroweak multiplet. The portal operators include $H^{\dagger}H$, $B^{\mu\nu}$, and HL. H is the Higgs doublet in Standard Model, $B^{\mu\nu}$ is the hypercharge field strength tensor, and L is a lepton doublet in Standard Model.

Because CEPC has a lot of powerful direct and indirect probes, it will play a crucial role in testing the Standard Model portals to dark matter.

Figure 12. Capacity of CEPC to probe dark photons. [33].

As shown in figure 12, CEPC covered the direct searches probe $\epsilon \subset (3 \times 10^{-4} - 10^{-3})$ depending on m_{Z_D} in the entire mass range up to 250 GeV.

5. Conclusion

The basic concepts of dark matter, the massive Hadron Collider (LHC), and circular electron-positron colliders are introduced in this paper (CEPC). The main characteristics of dark matter and the proof for its existence were initially covered in the study. There was a brief discussion of the theories used to explain dark matter. Dark halos and three different dark matter profiles were presented. The basic LHC setup, hypotheses, and the results that using the LHC to discover dark matter can produce were then introduced. This involves reducing the WIMP territory, bump hunting, and missing momentum signals. The advantages of CEPC in detecting dark matter were introduced in the final section.

Reference

[1]   NASA. (n.d.). Dark Energy, dark matter. NASA. Retrieved November 30, 2022, from https://science.nasa.gov/astrophysics/focus-areas/what-is-dark-energy

[2]   Bertone, G., & Hooper, D. (2018). History of dark matter. Reviews of Modern Physics, 90(4), 045002.

[3]   Lundmark, K. (1930). Über die Bestimmung der Entfernungen, Dimensionen, Massen und Dichtigkeit fur die nächstgelegenen anagalacktischen Sternsysteme. Meddelanden fran Lunds Astronomiska Observatorium Serie I, 125, 1-13.

[4]   Dark matter. CERN. (n.d.). Retrieved November 30, 2022, from https://home.cern/science/physics/dark-matter

[5]   Volders, L. M. J. S. (1959). Neutral hydrogen in M 33 and M 101. Bulletin of the Astronomical Institutes of the Netherlands, 14, 323.

[6]   Bosma, A. (1978). The distribution and kinematics of neutral hydrogen in spiral galaxies of various morphological types (Doctoral dissertation, Rijksuniversiteit te Groningen.).

[7]   Rubin, V. C., Ford Jr, W. K., & Thonnard, N. (1978). Extended rotation curves of high-luminosity spiral galaxies. IV-Systematic dynamical properties, SA through SC. The Astrophysical Journal, 225, L107-L111.

[8]   Mario De Leo (CC BY-SA 4.0), adapted from Corbelli, E., &Salucci, P. 2000, MNRAS, 311, 44.

[9]   Vallée, J. P. (2005). The spiral arms and interarm separation of the Milky Way: An updated statistical study. The Astronomical Journal, 130(2), 569.

[10] Clowe, D., Bradač, M., Gonzalez, A. H., Markevitch, M., Randall, S. W., Jones, C., & Zaritsky, D. (2006). A direct empirical proof of the existence of dark matter. The Astrophysical Journal, 648(2), L109.

[11] Bertone, G., & Tait, T. M. (2018). A new era in the quest for dark matter. arXiv preprint arXiv:1810.01668.

[12] Gunn, J. E., & Gott III, J. R. (1972). On the infall of matter into clusters of galaxies and some effects on their evolution. The Astrophysical Journal, 176, 1.

[13] Navarro, J. F., Frenk, C. S., & White, S. D. (1997). A universal density profile from hierarchical clustering. The Astrophysical Journal, 490(2), 493.

[14] Merritt, D., Graham, A. W., Moore, B., Diemand, J., & Terzić, B. (2006). Empirical models for dark matter halos. I. Nonparametric construction of density profiles and comparison with parametric models. The Astronomical Journal, 132(6), 2685.

[15] Avila-Reese, V., Firmani, C., & Hernández, X. (1998). On the formation and evolution of disk galaxies: Cosmological initial conditions and the gravitational collapse. The Astrophysical Journal, 505(1), 37.

[16] McGaugh, S. S., De Blok, W. J. G., Schombert, J. M., De Naray, R. K., & Kim, J. H. (2007). The rotation velocity attributable to dark matter at intermediate radii in disk galaxies. The Astrophysical Journal, 659(1), 149.

[17] Zooming in on dark matter. Max-Planck-Gesellschaft. (2020, September 2). Retrieved November

30, 2022, from https://www.mpg.de/15312438/0831-ext0-064909-zooming-in-on-dark-matter

[18] Gaitskell, R. J. (2004). Direct detection of dark matter. Annual Review of Nuclear and Particle Science, 54(1), 315-359.

[19] Xiao, M., Xiao, X., Zhao, L., Cao, X., Chen, X., Chen, Y., ... & Zhu, Z. (2014). First dark matter search results from the PandaX-I experiment. Science China Physics, Mechanics & Astronomy, 57(11), 2024-2030.

[20] Slatyer, T. R. (2018). Indirect detection of dark matter. Theoretical Advanced Study Institute in Elementary Particle Physics: anticipating the next discoveries in particle physics, 297-353.

[21] Bertone, G. (Ed.). (2010). Particle dark matter: observations, models and searches. Cambridge University Press. pp.83-104.

[22] Ellis, J., Flores, R. A., Freese, K., Ritz, S., Seckel, D., & Silk, J. (1988). Cosmic ray constraints on the annihilations of relic particles in the galactic halo. Physics Letters B, 214(3), 403-412.

[23] Hooper, D. (2018). TASI lectures on indirect searches for dark matter. arXiv preprint arXiv:1812.02029.

[24] Brüning, O., Burkhardt, H., & Myers, S. (2012). The large hadron collider. Progress in Particle and Nuclear Physics, 67(3), 705-734.

[25] Evans, L. (2007). The large hadron collider. New Journal of Physics, 9(9), 335.

[26] Herr, W., & Muratori, B. (2006). Concept of luminosity.

[27] Myers, S., & Schnell, W. (1983). Preliminary performance estimates for a LEP proton collider (No. LHC-NOTE-1). SCAN-0008106.

[28] Asner, A. M., Picasso, E., Baconnier, Y., Hilleret, N., Schmid, J., Schönbacher, H., Gobel, K., Weisse, E., Brandt, D., Poncet, A., Hagedorn, D., Vos, L., Henke, H., Garoby, R., Häbel, E., Evans, L. R., Bassetti, M., Fassò, A., Barbalat, O., … Laurent, J. M. (1990, January 29). A feasibility study of possible options. CERN Document Server. Retrieved October 20, 2022, from https://cdsweb.cern.ch/record/152775

[29] Breaking new ground in the search for dark matter. CERN. (n.d.). Retrieved December 1, 2022, from https://home.cern/news/series/lhc-physics-ten/breaking-new-ground-search-dark-matter

[30] Blinov, N., Krnjaic, G., & Tuckler, D. (2021). Characterizing dark matter signals with missing momentum experiments. Physical Review D, 103(3), 035030.

[31] Kane, G., & Watson, S. (2008). Dark matter and LHC: What is the connection?. Modern Physics Letters A, 23(26), 2103-2123.

[32] Aad, G., Abajyan, T., Abbott, B., Abdallah, J., Khalek, S. A., Abdelalim, A. A., ... & Bansil, H. S. (2012). Observation of a new particle in the search for the Standard Model Higgs boson with the ATLAS detector at the LHC. Physics Letters B, 716(1), 1-29.

[33] CEPC Study Group. (2018). CEPC conceptual design report: Volume 1-accelerator. arXiv preprint arXiv:1809.00285.

[34] CEPC Study Group. (2018). CEPC Conceptual Design Report: Volume 2-Physics \& Detector. arXiv preprint arXiv:1811.10545.

[35] Djouadi, A., Maiani, L., Moreau, G., Polosa, A., Quevillon, J., \& Riquer, V. (2013). The post-Higgs MSSM scenario: habemus MSSM?. The European Physical Journal C, 73(12), 1-10.

[36] Fan, J., Reece, M., \& Wang, L. T. (2015). Precision natural SUSY at CEPC, FCC-ee, and ILC. Journal of High Energy Physics, 2015(8), 1-30.

[37] Cao, Q. H., Huang, F. P., Xie, K. P., \& Zhang, X. (2018). Testing the electroweak phase transition in scalar extension models at lepton colliders. Chinese Physics C, 42(2), 023103.

[38] Cai, C., Yu, Z. H., \& Zhang, H. H. (2017). CEPC precision of electroweak oblique parameters and weakly interacting dark matter: The fermionic case. Nuclear Physics B, 921, 181-210.

[39] Low, M., \& Wang, L. T. (2014). Neutralino dark matter at 14 TeV and 100 TeV. Journal of High Energy Physics, 2014(8), 1-29.